Petroleum Research 11 (2026) 556–573

Contents lists available at ScienceDirect

Petroleum Research

journal homepage: http://www.keaipublishing.com/en/journals/petroleum-research/

Fracture conductivity damage in shale oil reservoirs: Mechanism model and its impact on oil production

Liang Zhang[a,b,*], Runzhen Wu[a], Chuan He[c], Xiang Li[a], Yige Qi[a], Linchao Yang[d], Zilin Zhang[d]

[a] School of Petroleum Engineering, China University of Petroleum (East China), Qingdao, 266580, China
[b] Key Laboratory of Unconventional Oil & Gas Development, China University of Petroleum (East China), Qingdao, 266580, China
[c] Shangma Subdistrict Office of Chengyang District, Qingdao, 266112, China
[d] Shengli Oilfield, Sinopec, Dongying, 257000, China

A R T I C L E I N F O

Article history:
Received 23 May 2025
Received in revised form
18 November 2025
Accepted 21 November 2025
Available online 26 November 2025

Keywords:
Shale oil
Fracture conductivity
Stress sensitivity
Gel-breaking residue
Hydration and expansion
Damage mechanism

A B S T R A C T

Shale oil reservoirs often experience severe hydraulic fracture stress sensitivity and conductivity damage, leading to rapid production decline and low oil recovery. Understanding fracture damage mechanisms is crucial for optimizing stimulation and production strategies. This study established a novel conductivity damage model of hydraulic fracture incorporating stress sensitivity, gel-breaking residue deposition, and the process of shale particle hydration, expansion, shedding, and blockage. A sensitivity analysis was conducted by numerical simulation to evaluate the impact of different damage mechanisms on fracture conductivity and oil production. The simulation results indicate that different damage mechanisms have varying impacts on fracture conductivity and production. Stress sensitivity significantly reduces main fracture conductivity, but broken gel residue is the primary cause of oil production decline. In branch fractures, both stress sensitivity and broken gel residue decrease conductivity, with stress sensitivity having the greatest impact on production. Shale particle expansion and deposition can further impair fracture conductivity, while particle detachment and output help restore it. Oil production of branch fractures is more sensitive to conductivity damages. These insights can guide fracture design, fracturing fluid optimization, and production control. It is recommended to increase proppant concentration to mitigate the adverse effect of stress sensitivity on oil production, enhance the concentration of anti-swelling agents in the pre-slug of fracturing fluid to better protect branch fractures, and control drawdown pressure to prevent shale particles from detaching and depositing in the fractures.

1. Introduction

Shale oil is an important unconventional oil and gas resource (Chen et al., 2021; Liu and Zhang, 2015). Large-scale hydraulic fracturing is an efficient way to develop shale oil, but due to the poor properties of shale reservoirs, high initial production, fast production decline, and low primary recovery often occur in the shale oil development process mainly because of various damage mechanisms of fracture conductivity (Ding, 2013; He et al., 2022; Liu et al., 2022).

To investigate the mechanisms of fracture conductivity damage, extensive laboratory experiments and modeling studies have been conducted. In the experimental aspect, most experiments focus on the stress sensitivity of fractures and its influencing factors (Ahamed et al., 2021; Chalmers et al., 2012; Cho et al., 2013; Jia, 2014; Kong et al., 2022; Li et al., 2016, 2019; Reyes and Osisanya, 2002; Shi and Sun, 2001; Sun, 2013; Wang et al., 2020a, 2020b; Xue et al., 2019). Early studies demonstrated that shale fracture permeability decreases exponentially with confining pressure, exhibiting stress sensitivity dependent on lithology and rock properties (Chalmers et al., 2012; Cho et al., 2013; Reyes and Osisanya, 2002; Shi and Sun, 2001). Cyclic loading can cause irreversible conductivity damage, while heterogenous shale exhibits intermediate sensitivity between high and low-

* Corresponding author. School of Petroleum Engineering, China University of Petroleum (East China), Qingdao, 266580, China.
E-mail address: zhlupc@upc.edu.cn (L. Zhang).
Peer review under the responsibility of Editorial Office of Petroleum Research.

https://doi.org/10.1016/j.ptlrs.2025.11.003
2096-2495/

permeability layers (Kong et al., 2022; Sun, 2013). The fracture stress sensitivity is also affected by proppant related factors. The damage mechanisms of different types of proppant and their effects on fluid flow are usually different, which can be elucidated using CT scanning (Ahamed et al., 2021). Under a low sand-laying concentration, the conductivity of fracture with coated sand is larger than that of ceramsite which is further larger than that of quartz sand (Jia, 2014). If the proppant particles are crushed, the small debris can migrate and deposit in fractures which can cause fracture conductivity decrease (Li et al., 2016). Fracture conductivity impairment induced by proppant migration correlates strongly with closure pressure and flow velocity (Wang et al., 2020a,b). In addition, fluid injection can also affect the fracture stress sensitivity. Some researchers investigated the impact of gel-breaker and its residues on fracture conductivity. The results showed that proppant crushing rate increased due to breaker soaking, proppant embedding was enhanced by fluid-formation interaction, and pore throat diameter was reduced because of fracturing fluid residues (Wang et al., 2020a,b). From the above, it can be seen that the stress sensitivity of shale fractures is affected by different factors. The damages induced by confining pressure, rock properties, and proppant related factors have been well revealed, but researches on the damages caused by gel-breaking fluid and shale particle detachment in fractures are relatively scarce.

Based on experimental results, a large number of studies have been conducted to establish fracture damage models using different methods to describe the deformation of rock and proppants in fractures (Cui et al., 2022; Jiao et al., 2022; Katende et al., 2023; Li et al., 2017; Liu et al., 2016; Peng et al., 2023; Yin et al., 2025; Zhang et al., 2015). Early studies mainly adopted the method of mathematical modeling for research. Zhang et al. (2015) developed an integrated fracture conductivity model incorporating mechanical properties of proppant and formation, and fracture design variables. Liu et al. (2016) created a two-step homogenization model for deformable rocks, capturing fracture permeability changes from anisotropic damage and nonlinear deformation. Li et al. (2017) established a constitutive model to predict proppant deformation and fracture permeability evolution under loading path. In recent years, the models have evolved towards fluid-solid coupling, using the finite element method to more intuitively depict and analyze the behavior of fracture damage. Jiao et al. (2022) developed a pore-scale thermal-hydraulic-mechanical (THM) coupled model for precise fluid-solid boundary interactions and damage-dependent conductivity. Cui et al. (2022) formulated a semi-analytical model for multi-well pads with heterogeneous fracture networks, revealing flow mechanisms in partially propped fractures with stress sensitivity. Peng et al. (2023) proposed a time-dependent conductivity model integrating shale creep effects using fractional calculus theory, and the simulation results indicated that production decline rates considering shale creep exceeded twice those accounting solely for proppant deformation and embedding. Yin et al. (2025) developed a global embedded proppant mesh model using Abaqus software demonstrating strong conductivity-closure stress sensitivity through dynamic proppant behavior analysis. From the above, it can be seen that these models mainly use mathematical or finite element simulation methods to describe the influence of rock deformation and proppant fragmentation and embedding in fractures. Some studies have also investigated the influence fracture damage on production capacity. No model has been found that describes the damage caused by gel-breaking liquid and shale particle detachment and its impact on production capacity.

To sum up, it can be concluded that in shale oil reservoirs, the damage to the fracture conductivity not only includes the widely discussed stress sensitivity (mainly a rock mechanics issue), but also the influence of injected fluids on the fracture conductivity cannot be ignored. This is determined by the special rock properties of oil shale, especially since oil shale contains a large amount of clay minerals, the gel-breaking residue can be adsorbed on the surface of shale particles, and shale particles are prone to expansion and detachment, resulting in a decrease in fracture conductivity. This process involves a chemical reaction issue during the rock-fluid interaction. It is difficult to integrate stress sensitivity and chemical damage into a single model for description, as a result, most of current studies just focus on the former. This highlights a critical need to develop a more comprehensive fracture damage model.

In this study, a novel numerical simulation model was developed to characterize the fracture conductivity damage mechanisms in shale oil reservoirs. The model integrates three key damage processes: fracture stress sensitivity, deposition of gel-breaking residue, and the hydration-expansion-shedding-deposition-blockage process of shale particles. Based on a single-fracture geologic model, the impacts of these damage mechanisms on fracture conductivity and oil production were evaluated individually and coupledly through numerical simulations. The comprehensive damage performance in fractures of shale oil reservoirs were revealed. This research can enhance the understanding of fracture damage in shale oil reservoirs and can provide theoretical support for optimizing fracturing parameters and implementing effective strategies to improve oil recovery.

2. Development and geological background

Shengli Oilfield is located in the Jiyang Depression of Bohai Bay Basin China. In 2008, researchers in Shengli Oilfield started systematically to prove the shale oil in Es3 formation of Bohai South Depression, and deployed the first shale oil exploratory well. By the end of 2018, 68 shale oil wells had been tested, and the initial production of 40 wells reached the industrial oil and gas flow standard, with a cumulative oil of nearly 120,000 tons. In recent years, Shengli Oilfield made another general deployment to strive for commercial breakthroughs. A number of shale oil wells, such as YYP-1, FYP-1, NX-55, and BY-5HF, were deployed for pilot tests, and drilling, fracturing, and development were implemented. The oil production of most of the wells, such as NX-55, was high at the beginning after fracturing, but it decreased quickly due to the impact of frequent well shut-ins and pressure releases. The seepage capacity of the matrix of the limy shale oil reservoir is poor, and the production capacity of the well is mainly determined by the reservoir transformed volume by fracturing. Whether the effective communication between the fracture system and shale matrix can be maintained for a long time is critical. Two aspects are still poorly understood. The first is the matching of the fracture conductivity and morphology with the shale matrix, and the second is the damage mechanism of the fracture conductivity (Ci et al., 2020).

The NX-55 well is located in the Niuzhuang depression of Dongying sag (Fig. 1). The shale oil bearing layer is in the Sha-4 formation, with a burial depth of 3400–3700 m. The reservoir temperature and pressure are 145 °C and 59.46 MPa (the pressure coefficient is 1.7), respectively. The porosity of the shale matrix is 6.7%, and the permeability is lower than 0.02 md. Under the reservoir condition, the initial oil saturation is 0.779, and the oil viscosity and density are 18 mPa s and 0.835 g/cm^3, respectively, while under the surface condition, the oil viscosity and density are 50 mPa s (at 50 °C) and 0.89 g/cm^3, respectively, and the ratio of dissolved gas and oil is 38 m^3/t. The well adopted a segmented fracturing completion method using fully soluble bridge plugs and

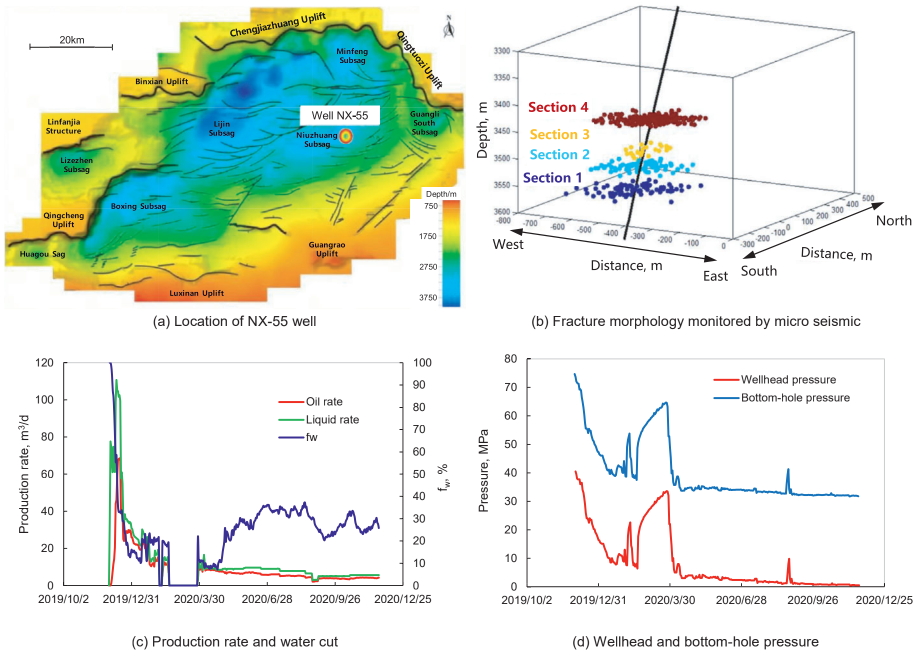

Fig. 1. Location, fracture morphology and production dynamic of NX-55 well.

suspended integrated fracturing fluid. Four hydraulic fracturing stages were carried out vertically, with 205 m^3 of proppant and 3777 m^3 of fracturing fluid. 180–200t of CO_2 was pre-injected in each stage for energy enhancement and fracture expansion. Microseismic monitoring showed that the half length of the fracture is 150–180 m, the fracture height is 20–31 m, and the fractured formation volume is 1.459 million m^3. According to the design, the major fracture should have a conductivity of 12–70 D·cm, while the branch fracture has a conductivity of 0.5–12 D·cm. After the fracturing operation was completed, the shale formation near the well was severely pressurized, and the wellhead pressure reached up to 40 MPa. With the production, the wellhead pressure gradually decreased. The initial liquid production rate reached 110 m^3/d, with a high water cut. After one month, the liquid production rate decreased to 30 m^3/d, and the water cut decreased to 20%. After continuing production for 1.5 months, the well was shut in for over a month, during which the wellhead pressure was restored significantly. Then, the well was opened for 8 months of production, but as production, the wellhead pressure rapidly decreased to 5 MPa at the beginning and slowly decreased to 0.5 MPa. The corresponding fluid production rate gradually decreased from 13 m^3/d to 5.6 m^3/d. The water cut first decreased and remained at around 10% due to the imbibition effect of fracturing fluid in the fractures during the shut-in period, but one month later, the water cut rose and fluctuated between 20% and 35%. This may be due to the fracture compression caused by the decrease in formation pressure, which can increase movable water saturation and decrease fracture conductivity. These are worth conducting in-depth research on the fracture damage mechanism.

3. Numerical simulation model

3.1. Damage mechanism model of fracture conductivity

In the process of shale oil production by depressurization after hydraulic fracturing, the conductivity of the fracture is mainly affected by the fracture stress sensitivity, the deposition of the gel-breaking residue, and the hydration-expansion-shedding-deposition-blockage process of shale particles. The establishment process of the damage mechanism model of fracture conductivity is as follows.

3.1.1. Damage of fracture conductivity induced by stress sensitivity

Major and branch fractures are formed during the hydraulic fracturing process in shale oil reservoirs. Major fractures, with high sanding concentration and conductivity, are directly connected to the wellbore. Branch fractures, with relatively low sanding concentration and conductivity, are used to connect the major fractures and shale matrix, which plays a bridge effect. The stress sensitivity of matrix and fracture can be characterized using the porosity ratio (φ/φ_o) and permeability ratio (K/K_o) relationship table. When the formation pressure decreases, the porosities of the matrix and fracture are compressed and reduced, and the permeabilities will also decrease correspondingly. The stress sensitivities of the shale matrix and fracture have been measured before using the real cores sampled from the NX-55 well (Meng et al., 2021). It was assumed that the pore compressibility of the matrix and fractures was the same, both at 8×10^{-6} 1/kPa, and the initial effective confining pressure was 5 MPa. The confining pressures corresponding to the porosity ratio φ/φ_o in the range of 0.7–1 were calculated. Then according to these confining pressures, displacement experiments were conducted to measure the core matrix permeability and fracture conductivity, and corresponding K/K_o was calculated. For simplification, the ratio of fracture permeability was assumed to be the ratio of fracture conductivity. The experimentally measured initial matrix permeability ranges from 0.0221 to 0.1146 md, with proppant concentrations of 8–10 kg/m^2 for the main fractures and 1–5 kg/m^2 for the branch fractures. Based on the experimental results, a typical φ/φ_o and K/K_o relationship table of shale matrix, branch fracture, and major fracture was designed for this numerical simulation study, as shown in Table 1. It can be seen that under the same φ/φ_o, the K/K_o of shale matrix is the largest, the K/K_o of major fracture is followed, and the smallest one is the K/K_o of branch fracture, which

Table 1
Relationship between φ/φ_o and K/K_o of the shale matrix, major fracture, and branch fracture.

Matrix		Major fracture		Branch fracture	
φ/φ_o	K/K_o	φ/φ_o	K/K_o	φ/φ_o	K/K_o
0.70	0.66	0.70	0.25	0.70	0.001
0.75	0.76	0.75	0.55	0.75	0.009
0.80	0.79	0.80	0.60	0.80	0.020
0.85	0.82	0.85	0.70	0.85	0.100
0.90	0.85	0.90	0.80	0.90	0.500
0.95	0.93	0.95	0.90	0.95	0.700
1.00	1.00	1.00	1.00	1.00	1.000

mean the shale matrix has the weakest stress sensitivity, while the branch fracture has the stongest one. Referring to this φ/φ_o and K/K_o relationship table, in the process of depressurization for production, the cumulative oil in the major fracture will decrease by 10.5%. In comparison, the cumulative oil in the branch fracture will decrease by 68.3% (the original formation pressure is 59.46 MPa, and the minimum bottom hole flow pressure is 20 MPa).

3.1.2. Damage of fracture conductivity induced by gel-breaking residue

During hydraulic fracturing, under the effect of injection pressure difference, the fracturing fluid immerses into the fracture and its adjacent matrix to form gel-breaking residues. It undergoes deposition, which has an important impact on fracture conductivity and shale oil production. An equivalent chemical reaction equation for the deposition of the gel-breaking residue was constructed to describe this process, as shown in Eqs. (1) and (2). It is hypothesized that during the injection of the fracturing fluid and the well shut-in period, the gel-breaking residues in the aqueous phase gbw(w) will be converted into solid-phase deposits gbs(s) when the gel-breaking fluid encounters the matrix minerals Ms(s) in and near the fracture. It can lead to a decrease in the permeability of the fracture and the nearby matrix. Some laboratory experiments showed that when the concentration of gel-breaking residue increased from 50 mg/L to 700 mg/L, the fracture conductivity damage factor increased from 5%-10% to 60%–95% (Ni et al., 2016). Therefore, under the basic parameter settings, an average concentration of 300 mg/L of gel-breaking residue was assumed, and the permeability damage factor of gel-breaking residue to the fracture and nearby matrix was set to be 40%–65%. The damage to porosity and permeability of the matrix and fracture induced by gel-breaking residue also follow the φ/φ_o and K/K_o table, as shown in Table 1. The other model parameters are shown in Table 2 gbw(w) and gbs(s) are derived from polymers, therefore, their molecular weights were assumed to be a typical value of 8000 g/mol. The deposition process of gbw(w) is primarily controlled by the reaction frequency factor f_1 and is not influenced by activation energy E_1. Hence, E_1 was assumed to be 0, and f_1 was determined to be 1×10^{-6} by matching the 40%–65% permeability damage caused by 300 mg/L of gel-breaking residue (see section 4.2.1, at 0.03 wt% of gel-breaking residue, the conductivity of the major fracture decreases by 40% from 3.57D·cm to 2.14 D·cm, while the conductivity of the branch fracture decreases by 65% from 0.57D·cm to 0.20D·cm compared with the case of only stress-sensitivity).

Table 2
Basic parameter settings of the deposition reaction model of gel-breaking residue.

Parameters	Values
Molecular weight of gbw(w), g/mol	8000
Molecular weight of gbs(s), g/mol	8000
Density of gbs(s), kg/m^3	1500
Molecular weight of Ms(s), g/mol	150
Density of Ms(s), kg/m^3	2650
Deposition reaction frequency factor of gel-breaking residue, f_1, 1/s	1×10^{-6}
Deposition reaction activation energy of gel-breaking residue, E_1, J/mol	0

$$gbw(w) + Ms(s) \rightarrow gbs(s) + Ms(s) \tag{1}$$

$$K_1 = f_1 \exp\left(-\frac{E_1}{RT}\right)\left(\varphi_f \rho_w S_w x_{gbw}\right) \tag{2}$$

where K_1 is the deposition reaction rate of gel-breaking residue, $mol/(s{\cdot}m^3)$; f_1 is the reaction frequency factor, 1/s; E_1 is the reaction activation energy, J/mol; R is the gas constant, 8.34 J/(mol·K); T is the temperature, K; φ_f is the fluid porosity (the ratio of the pore volume occupied by the fluid to the volume of the rock), fraction; ρ_w is the aqueous-phase molar density, mol/m^3; S_w is the aqueous-phase saturation, fraction; x_{gbw} is the concentration of gel-breaking residue in aqueous phase, mole fraction.

3.1.3. Damage of fracture conductivity induced by shale particles

Due to the presence of clay minerals in shale oil reservoirs, the fracture may show a strong hydration expansion phenomenon during the hydraulic fracturing process, which leads to a decrease in fracture conductivity. If the hydrated and expanded shale particles on the fracture wall can be shed during the blowout and backflow process of fracturing fluid, the shale particles may be deposited in the fracture to form a blockage or discharged with the fracturing fluid. Hence, the presence of clay minerals has an uncertain influence on the fracture permeability. For the damage caused by the shale particles in the fracture, three reaction equations were defined to describe the hydration-expansion-shedding-deposition-blockage process of shale particles.

(1) **Reaction of hydration and expansion of shale particles.** Generally, the concentration of the anti-swelling agent in the fracturing fluid decides the degree of shale hydration and expansion. Hence, it is assumed that the initial content of shale particles involved in hydration and expansion can be defined according to the concentration of the anti-swelling agent, which further determines the upper limit of the porosity reduction of the hydrated shale rocks. A local equilibrium reaction equation was established to describe the hydration and expansion process of shale particles. When the concentration of the anti-swelling agent reaches high enough, the shale particles will not be hydrated and expanded. The specific equivalent reaction equations are shown in Eqs. (3)–(5), where Mshs(s) and Msshs(s) are the shale particles before and after hydration and expansion, respectively, and hsw(w) is the anti-expansion agent.

$$Mshs(s) + hsw(w) \rightarrow Msshs(s) + hsw(w) \tag{3}$$

$$K_2 = f_2 \exp\left(-\frac{E_2}{RT}\right)\left(\varphi C_{Mshs}\right)\left(\varphi_f \rho_w S_w \Delta x_{hsw}\right) \tag{4}$$

$$\Delta x_{hsw} = max(0, x_{eq} - x_{hsw}), \frac{1}{x_{eq}} = k(p,T) = \left(\frac{k_1}{p} + k_2 p + k_3\right) exp\left(\frac{k_4}{T}\right) \tag{5}$$

where K_2 is the hydration and expansion reaction rate of shale particles, mol/(s·m^3); f_2 is the reaction frequency factor, m^3/(s·mol); E_2 is the activation energy of the reaction, J/mol; φ is the formation porosity, fractional; C_{Mshs} is the concentration of shale particles before hydration and expansion, mol/m^3; Δx_{hsw} is the reaction driving force of shale hydration and expansion induced by the insufficient concentration of the anti-swelling agent, mole fraction; x_{eq} is the critical equilibrium concentration of the anti-swelling agent when the hydration expansion of shale is just completely suppressed, mole fraction; x_{hsw} is the concentration of the anti-swelling agent, mole fraction; p is the pressure, kPa; and k_i is the correlation constant, dimensionless.

(2) **Reaction of shedding of shale particles.** During the blowout and backflow process of fracturing fluid, when the water phase flow rate inside the fracture exceeds the critical start-up flow rate, the hydrated and expanded shale particles Msshs(s) inside the fracture and on the fracture wall surface will be shedded. Shale particles sandw(w) will be generated and transported with the liquid phase. The specific reaction equations are shown in Eqs. (6) and (7):

$$Msshs(s) \rightarrow sandw(w) \tag{6}$$

$$K_3 = f_3 \exp\left(-\frac{E_3}{RT}\right)(\varphi C_{Msshs})\left(\frac{V_w - V_{cfs}}{V_{ref}}\right) \tag{7}$$

where K_3 is the shedding reaction rate of hydrated and expanded shale particle, mol/(s·m^3); f_3 is the reaction frequency factor, 1/s; E_3 is the reaction activation energy, J/mol; C_{Msshs} is the concentration of hydrated and expanded shale particles, mol/m^3; V_w is the water phase flow rate, m/s; V_{cfs} is the critical water flow rate of shale particle starting to shed, m/s; V_{ref} is the reference flow rate, m/s.

(3) **Reaction of deposition and blockage of shale particles.** If the shed shale particles in the water phase are deposited in the fracture, it can cause a decrease in the fracture permeability. The deposited shale particles are named sandde(s), and the specific reaction equations are shown in Eqs. (8) and (9):

$$sandw(w) \rightarrow sandde(s) \tag{8}$$

$$K_4 = f_4 \exp\left(-\frac{E_4}{RT}\right)\left(\varphi_f \rho_w S_w x_{sandw}\right) \tag{9}$$

where K_4 is the deposition reaction rate of shed shale particles to plug the fracture, mol/(s·m^3); f_4 is the reaction frequency factor, 1/s; E_4 is the reaction activation energy, J/mol; and x_{sandw} is the concentration of shale particles in the aqueous phase, mole fraction.

Combining the results of indoor experiments and literature research, the basic parameter settings of the hydration-expansion-shedding-deposition-blockage damage mechanism model of shale particles are determined, as shown in Table 3. For the hydration-expansion reaction, the relationship between the expansion rate of shale particles and the anti-swelling agent concentration was fitted according to the results of indoor experiments (Meng et al., 2021), as shown in Fig. 2. It can be seen that when the concentration of the anti-swelling agent is greater than 2.7 wt%, the expansion rate of shale particles will drop to 0%. The contents of shale particles that can be hydrated and expanded at different anti-swelling agent concentrations were calculated and given in Table 4. The original density of shale particles was assumed to be 2650 kg/m^3. After hydration, their density decreased to 1325 kg/m^3 while their volume doubled. Under the reservoir conditions, the expansion volume of shale particles mainly occupies the pore volume. Hence, the ratio of porosity reduction to initial porosity is approximatively equal to the ratio of expansion rate to initial porosity. The ratio of porosity before and after expansion is equal to 1 minus the ratio of expansion rate to initial porosity. Then, the decrease rate of fracture permeability can be calculated according to the relationship table of φ/φ_o and K/K_o as shown in Table 1. In addition, the 2.7 wt% was selected as the critical equilibrium concentration of the anti-swelling agent to suppress the hydration expansion of shale particles completely. The parameters used for x_{eq} were determined to be $k_1 = k_2 = k_4 = 0$ and $k_3 = 37.04$. For the shedding reaction of shale particles, the reaction frequency factor and critical flow rate were determined by parameter trial calculation to make that the shedding process of the hydrated and expanded shale particles from the fracture wall was just enough to restore the permeability of the fracture and the nearby matrix to the original level. For the deposition and blockage reaction of shale particles, the reaction frequency factor was also determined by parameter trial calculation to make sure that the shedding shale particles just can not be deposited in the fracture for blockage.

It should be pointed out that the most fundamental aspect of these damage mechanisms is their impact on porosity, which subsequently leads to the change of permeability. Hence, for simplification, a uniform φ/φ_o and K/K_o relationship table was used for these damage mechanisms. If the damage occurs in the matrix, it follows the matrix porosity-permeability relationship. If it occurs in the fracture, it follows the fracture porosity-permeability relationship. This approach enables the coupling of various damage mechanisms in a same system.

Table 3
Basic parameter settings of damage mechanism model of shale particles.

Parameter	Value	Parameter	Value
Molecular weight of Mshs(s), g/mol	2650	Frequency factor of hydration-expansion reaction, f_2, m^3/(s·mol)	0.001
Density of Mshs(s), kg/m^3	2650	Activation energy of hydration-expansion reaction, E_2, kJ/mol	0
Molecular weight of Msshs(s), g/mol	2650	Frequency factor of particle shedding reaction, f_3, m^3/(s·mol)	0.001
Density of Msshs(s), kg/m^3	1325	Activation energy of particle shedding reaction, E_3, kJ/mol	0
Molecular weight of sandw(w), g/mol	2650	Critical water flow rate of particle shedding, V_c, m/d	0.01
Density of sandw(w), kg/m^3	1325	Reference flow rate, V_{ref}, m/d	0.01
Molecular weight of sandde(s), g/mol	2650	Frequency factor of particle deposition reactions, f_4, m^3/(s·mol)	0.001
Density of sandde(s), kg/m^3	1325	Activation energy of particle deposition reaction, E_4, kJ/mol	0

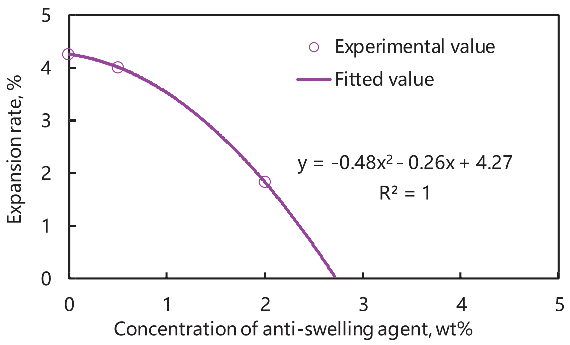

Fig. 2. Fitting result of the relationship between the expansion rate of shale particles and the concentration of anti-swelling agent.

Table 4
Contents of shale particles that can be hydrated and expanded at different anti-swelling agent concentrations.

Concentration of anti-swelling agent, wt%	Expansion rate of shale particles, %	Porosity ratio before and after damage	Content of shale particle for hydration expansion, mol/m^3
0.0	4.27	0.3627	100.0
0.5	4.02	0.4000	94.1
1.0	3.53	0.4729	82.7
1.5	2.81	0.5814	65.7
2.0	1.83	0.7254	43.1
3.0	0.00	1.0000	0.0
5.0	0.00	1.0000	0.0

3.2. Numerical simulation model of a single fracture

Horizontal wells with segmental fracturing are often used to develop shale oil reservoirs. To conveniently study the damage mechanisms of fracture conductivity and their impacts on shale oil production, only one fracture of the horizontal well section was selected as the research object to build the geological model, as shown in Fig. 3. Hence, a conceptual numerical simulation model of a single fracture was established using the STARS model of the software CMG. The main parameter settings of the model are shown in Table 5, which refers to the shale oil reservoir conditions of the NX-55 well in Shengli Oilfield. The size of the geological model is 60 m $\times$ 240 m $\times$ 30 m, the grid size is uniform, namely 3 m $\times$ 3 m $\times$ 30 m, and the grid number is 20 $\times$ 80 $\times$ 1 = 1600. A fracture with a length of 180 m extends from the middle to the side of the model along the J direction. The grids where the fracture is located were refined symmetrically along the I direction. The center refined grid with a width of 0.6 cm stands for the fracture. The fracture conductivity was discussed in two cases. When it stands for the major fracture, the conductivity was set to be 60 D·cm; when it stands for branch fracture, the conductivity was set to be 1 D·cm. According to the situation when a hydraulic fracturing is just finished, 0.03 wt% of gel-breaking residue and 2.0 wt% of anti-swelling agent were defined in the water phase in the fracture and the nearby matrix (the two refined grids near the fracture) at the beginning of simulation. Once the simulation starts, the reactions of these chemical agents will also start. The shale matrix and fracture were assigned different φ/φ_o and K/K_o relationship tables (Table 6). It is assumed that the damage of permeability caused by the deposition of gel-breaking residue and the hydration-expansion-shedding-deposition-blockage process of shale particles also follow the relationship table. In addition, the horizontal well adopts a constant flow rate of 10 m^3/d for production. When the flow rate of 10 m^3/d cannot be maintained, it will switch to produce with a constant bottom-hole flow pressure of 20 MPa. The production period was set to be 10 years.

Sensitivity analysis scheme of influencing factors affecting fracture conductivity and oil production is shown in Table 7, in which the values marked with the superscript "*" are under the basic conditions. When the sensitivity analysis of a certain parameter is carried out, the rest parameters take the values under the basic conditions. The first column in the table is the number of the damage mechanisms to be evaluated, and the last column is labeled with the number of the damage mechanisms activated in the simulation model. When the damage of fracture stress sensitivity is evaluated, only the φ/φ_o and K/K_o relationship table was activated in the model. Based on the damage of the stress sensitivity, the damages of gel-breaking residue and shale particles were further evaluated separately, and the corresponding mechanisms were activated in the model. Finally, the damage changes to the fracture conductivity and oil production were evaluated when more and more damage mechanisms are involved.

4. Simulation results and analysis

4.1. Influence of stress sensitivity on fracture conductivity and oil production

The effect of stress sensitivity on fracture conductivity and oil production was first evaluated. The oil production processes at two kinds of initial fracture conductivity (60D·cm for major fracture and 1D·cm for branch fracture) were simulated and compared with and without stress sensitivity. The changes of cumulative oils and conductivities in the middle of the fracture with time under different conditions are shown in Fig. 4, and the reservoir pressure and permeability fields after one year of production are shown in Fig. 5.

The results show that there is stress-sensitivity damage in major and branch fractures. Their cumulative oils decrease significantly compared with those without stress-sensitivity

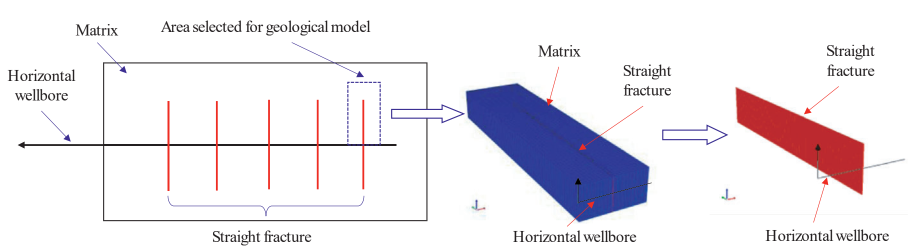

Fig. 3. Schematic diagram of the geologic model of the shale oil reservoir with a single fracture.

Table 5
Main parameter settings of the reservoir and fluid properties in the geological model.

Parameter	Value	Parameter	Value
Reservoir depth, m	3490	Reservoir temperature, °C	145
Reservoir thickness, m	30	Reservoir pressure, MPa	59.46
Size of the model, m^3	60 × 240 × 30	Initial water saturation, %	22.1
Size of the uniform grid, m^3	3 × 3 × 30	Dissolved gas-oil ratio, m^3/t	38
Number of grids	20 × 80 × 1	Oil density underground, g/cm^3	0.835
Porosity of the matrix, %	6.7	Oil viscosity underground, mPa·s	18
Permeability of the matrix, md	0.02	Oil density at surface, g/cm^3	0.890
Porosity of the fracture, %	30	Oil viscosity at surface, mPa·s	50
Conductivity of major fracture, μm^2·cm	60	Concentration of gel-breaking residue in fracturing fluid, wt%,	0.03
Conductivity of branch fractures, μm^2·cm	1	Concentration of anti-swelling agent in fracturing fluid, wt%	2.0
Fracture length, m	180	Liquid production rate, m^3/d	10
Fracture width, cm	60	The lowest bottom hole flow pressure, MPa	20
Fracture permeability, md	1000 or 16.7	Production time, year	10

Table 6
Data of oil-water and oil-gas relative permeability.

Oil-water Relative permeability			Oil-gas relative permeability		
S_w	k_{rw}	k_{row}	S_l	k_{rg}	k_{rog}
0.300	0.0000	1.000	0.410	0.397	0.000
0.350	0.0036	0.700	0.471	0.310	0.040
0.400	0.0096	0.450	0.541	0.220	0.110
0.450	0.0312	0.300	0.648	0.110	0.250
0.500	0.0708	0.160	0.748	0.055	0.410
0.550	0.1200	0.060	84.2	0.020	0.600
0.614	0.2064	0.014	94.8	0.005	0.840
0.650	0.2676	0.000	100.0	0.000	1.000

Table 7
Sensitivity analysis scheme of influencing factors affecting fracture conductivity and oil production.

No.	Assessed mechanism	Influencing factor	Values assessed	Mechanisms activated in the model
1	Stress sensitivity	Relationship between φ/φ_o and K/K_o	Considered*, not considered	1
2	Deposition of gel-breaking residue	Concentration of gel-breaking residue, wt%	0.01, 0.03*, 0.05, 0.08	1+2
		Water saturation in fractures and nearby fracture walls, %	22.1*, 32.1, 42.1, 52.1	
3	Hydration expansion of shale particles	Concentration of anti-swelling agent, wt%	0.0, 0.5, 1.0, 1.5, 2.0*, 3.0, 5.0	1+3
4	Shedding of shale particles	Shedding or not	shedding*, not shedding	1+3+4
5	Deposition and blockage of shale particles	Reaction frequency factor of shale deposition, m^3/s/mol	0, 0.001*, 0.010, 0.100	1+3+4+5
		Critical water flow velocity for shale shedding, m/d	0.001, 0.010*, 0.100, 1.000	
6	Damage mechanisms coupled	Coupling mode	1, 1+2, 1+2+3, 1+2+3+4, 1+2+3+4+5	Same as the left

damage. For the case of major fracture, the cumulative oil decreases from 7432 m^3 to 6654 m^3 by 10.5%, while for the case of branch fracture, the cumulative oil decreases from 4917 m^3 to 1560 m^3 by 68.3%. Hence, the oil production of branch fracture is more strongly damaged by the stress sensitivity.

In addtion, from the view of fracture conductivity change, because of the high conductivity, the pressure in the major fracture propagates faster than in branch fracture. Even though the conductivity of the major fracture decreases significantly due to stress sensitivity (from 60 D·cm to 3.57 D·cm by 94.05%), it still maintains a high level, which has a relatively small impact on the oil production, and the pressure drop range in the fracture does not change much. For the branch fracture, the initial fracture conductivity is small, and the stress sensitivity is strong. Because the initial permeability along the fracture was defined to be the same, the closer to the well, the greater the conductivity damage in the fracture caused by pressure drop. This, in turn, leads to the pressure drop not propagating easily to the deep part of the fracture. As a result, the pressure drop range in the fracture is small, and the conductivity at the middle of the fracture decreases relatively small (from 1 D·cm to 0.57 D·cm by 43%), but the cumulative oil of the fracture decreases significantly.

4.2. *Influence of gel-breaking residue on fracture conductivity and oil production*

Based on the fracture stress sensitivity, the damage mechanism of the gel-breaking residue depositing in fracture was further simulated and analyzed. Before the simulation, a certain concentration of gel-breaking residue was predefined in the water phase in the fracture and the nearby shale matrix. In this section, the influences of the gel-breaking residue concentration and the water

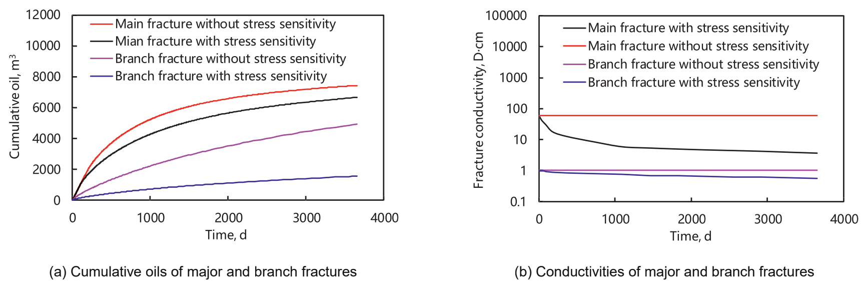

Fig. 4. Comparison of cumulative oils and fracture conductivities with and without stress-sensitivity.

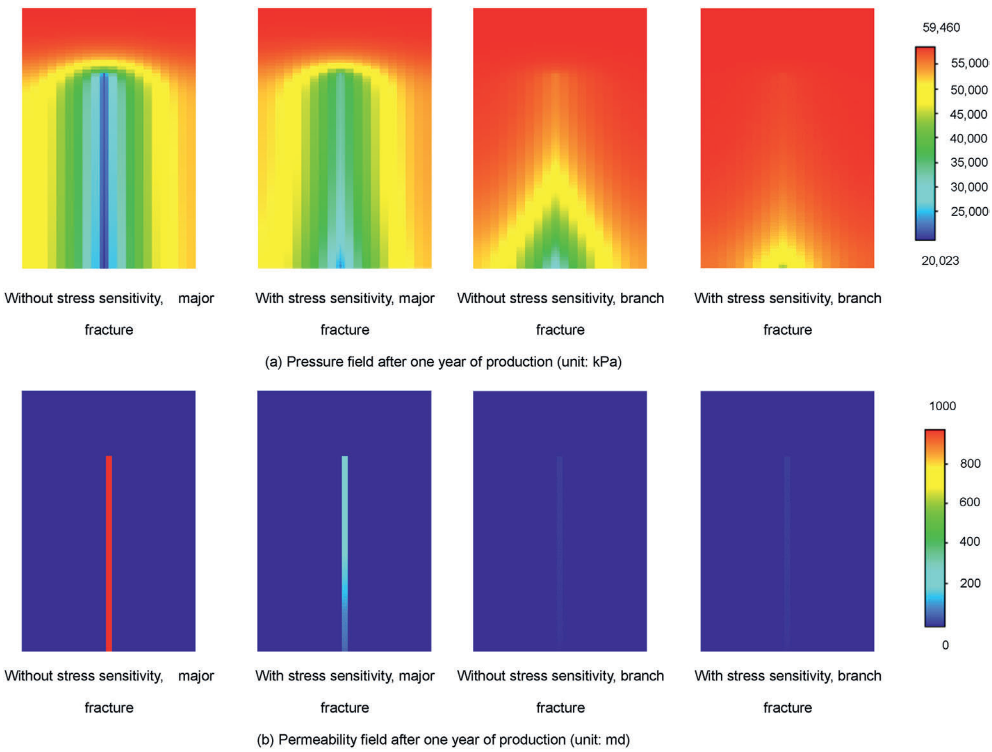

Fig. 5. Comparison of reservoir pressure and permeability fields with and without stress sensitivity.

saturation in the fracture and nearby shale matrix on the cumulative oil and fracture conductivity were assessed.

4.2.1. Influence of the concentration of gel-breaking residue

Under the basic condition of water saturation (22.1%), the cumulative oil and related fracture parameters were compared at different concentrations of gel-breaking residue in the formation water in the fracture and the nearby shale matrix. The results are shown in Figs. 6 and 7.

During the hydraulic fracturing process in the field, the incomplete gel breaking of the fracturing fluid can easily lead to the retention of the gel-breaking residue in the fracture during the flow back of the fracturing fluid. This process reduces the porosity of the fracture and damages the fracture permeability and conductivity. The greater the concentration of gel-breaking residue in formation water, the greater the amount of residue deposited, the greater the decrease in fracture conductivity, and the lower the oil production. Specifically, as the concentration of gel-breaking residue increases from 0 wt% to 0.08 wt%, the conductivity of major fracture (10 years of depressurization for production later) decreases by 49.58% from 3.57D·cm to 1.8D·cm, and the corresponding cumulative oil decreases by 45.18% from 6654 m^3 to 3648 m^3. Accordingly, for the branch fracture, the conductivity will decrease by 91.23% from 0.57D·cm to 0.05D·cm, and the cumulative oil decrease by 89.04% from 1560 m^3 to 171 m^3. Through comparison, it can be found that the branch fracture is more easily affected by the gel-breaking residue. The damage of ge-breaking residue to the conductivity and oil production of branch fracture is much greater than that of major fracture. In addition, it should be noted that during the fracturing fluid flow back, part of the gel-breaking residue without deposition in the matrix near the fracture will enter the fracture, which leads to the amount of the residue deposited in the fracture is slightly larger than that in the matrix near the fracture. The porosities of the fracture and the matrix decrease significantly, but the former is still higher than the latter.

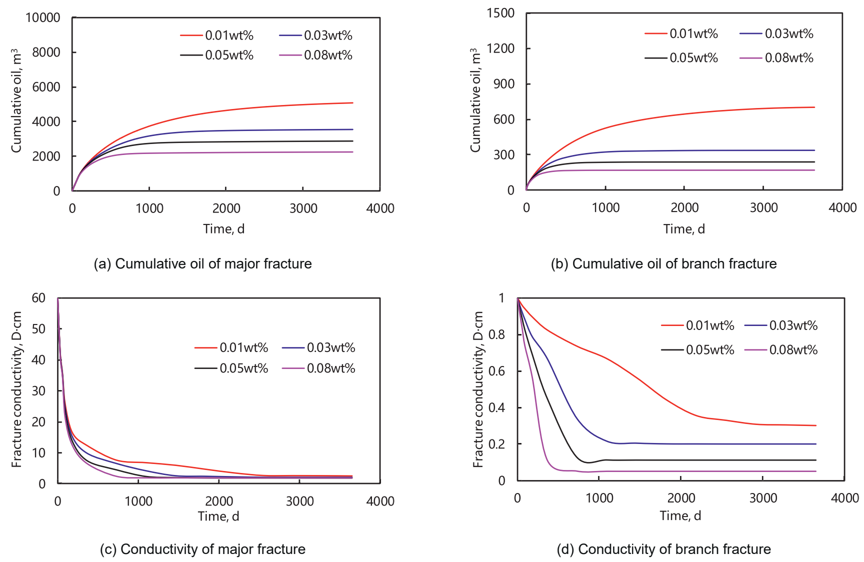

Fig. 6. Comparison of cumulative oils and fracture conductivities at different concentrations of gel-breaking residue in water.

4.2.2. Influence of the water saturation in fracture walls

Under the basic condition with a gel-breaking residue concentration of 0.03 wt%, the cumulative oil and related fracture parameters were compared at different water saturations in the fracture and the nearby shale matrix. The results are shown in Figs. 8 and 9.

The water saturation in the fracture and the nearby matrix represents the initial retention amount of the fracturing fluid in the shale oil reservoir. The greater the water saturation, the more gel-breaking residue is retained, and the greater the damage to fracture porosity and permeability. Specifically, with the water saturation in the fracture increasing from 22.1% to 52.1%, the conductivity of major fracture (10 years of production later) decreases by 9.52% from 2.1D·cm to 1.9D·cm, and the corresponding cumulative oil decreases by 11.46% from 3569 m^3 to 3160 m^3. Accordingly, the conductivity of branch fracture decreases by 15% from 0.2D·cm to 0.17D·cm, and the cumulative oil decreases by 74.63% from 339 m^3 to 86 m^3. The conductivity of major fractures generally decreases to the minimum value after 3.8 years of production, while the conductivity of branch fractures reaches the minimum value after 2.7 years of production. To sum up, the conductivity of branch fractures is more significantly affected by the water saturation in the fracture. The permeability of branch fractures is more sensitive to the change of porosity than that of major fractures. After 3 years of production at different water saturations, the contents of the gel-breaking residue in major fractures do not differ much.

4.3. Influence of shale particles on fracture conductivity and oil production

Based on the fracture stress sensitivity, the damage mechanism of hydration-expansion-shedding-deposition-blockage process of shale particles in the fracture was further simulated and analyzed. Before the simulation, in the fracture and the nearby shale matrix, a certain concentration of anti-swelling agent was predefined in the water phase, and a certain content of shale particles for hydration and expansion was predefined in the solid phase. In this section, the influence of the anti-swelling agent concentration, shedding or not, deposition reaction frequency factor, and critical water flow rate for particle shedding on cumulative oil and fracture conductivity were evaluated.

4.3.1. Influence of hydration and expansion of shale particles

The damage mechanism of hydration and expansion of shale particles in the fracture was simulated by presetting the content of the shale particles for hydration and expansion according to the concentration of the anti-swelling agent (referring to Table 4). The cumulative oil and related fracture parameters were compared at different concentrations of anti-swelling agent in the fracture and the nearby shale matrix. The results are shown in Figs. 10 and 11.

Through analysis, it can be seen that the lower the concentration of the anti-swelling agent, the more severe the hydration and expansion of the shale particles. With the decrease of the concentration of the anti-swelling agent, major fracture conductivity decreases by 61.90% from 3.57 D·cm to 1.36 D·cm, and the cumulative oil decreases by 30.27% from 6654 m^3 to 4640 m^3. For the branch fracture, the conductivity decreases by 84.21% from 0.57 D·cm to 0.09 D·cm, and the cumulative oil decreases by 74.36% from 1560 m^3 to 400 m^3. Overall, a higher concentration of anti-swelling agents is more favorable to inhibiting the expansion of shale. When the concentration of the anti-swelling agent is larger than 3 wt%, there is almost no hydration and expansion of shale particles in the fracture, and the fracture conductivity is mainly damaged by the stress sensitivity.

The typical concentration of anti-swelling agent used in the hydraulic fracturing fluid in shale oil reservoirs in Shengli Oilfield is 2 wt%. The expansion rate of shale is 1.83%, and the content of expandable shale particles is 43.1 mol/m^3. The porosity of the fracture and the nearby matrix is reduced by 27% after the hydration and expansion of shale particles. Compared with the case without shale hydration and expansion, the conductivity of major fracture decreases by 21.57% from 3.57 D·cm to 2.80D·cm, while the conductivity of branch fracture decreases by 19.30% from 0.57 D·cm to 0.46D·cm, and the effect of the anti-swelling agent is relatively better for branch fracture.

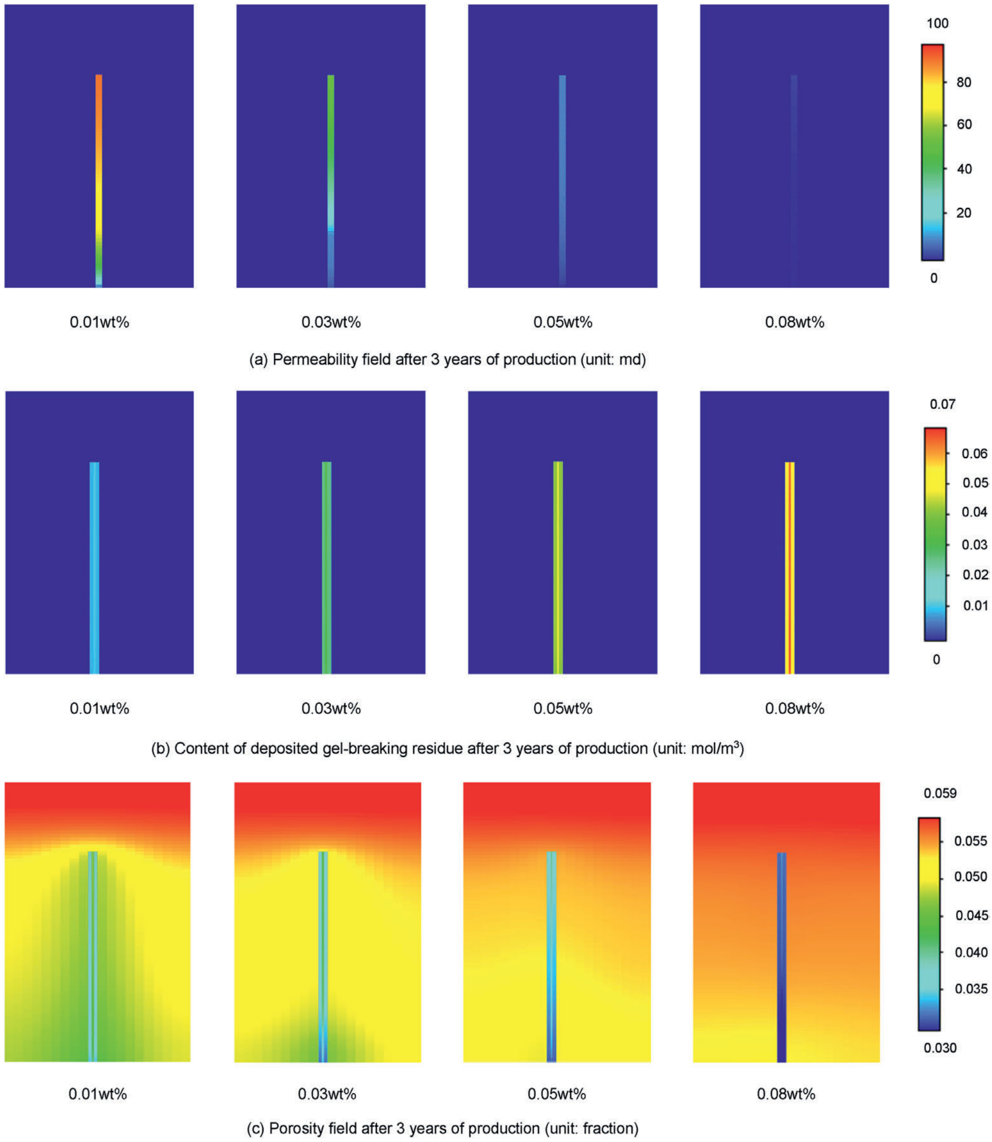

Fig. 7. Comparison of reservoir permeabilities, porosities, and contents of deposited gel-breaking residue at different concentrations of gel-braking residue in water (taking major fracture as an example).

4.3.2. Influence of shedding of hydrated and expanded shale particles

Based on the hydration and expansion of shale particles, the damage mechanism of the shale particle shedding was further simulated and analyzed. The cumulative oil and related fracture parameters were compared with and without shale particle shedding at different concentrations of the anti-swelling agent in the fracture and the nearby shale matrix. The results are shown in Figs. 12 and 13.

Through analysis, it can be found that when the concentrations of the anti-swelling agent are 0 wt% and 2 wt%, the shale expansion rates are 4.27% and 1.83%, respectively, and the contents of expandable shale particles are 100 mol/m^3 and 43.1 mol/m^3, respectively. For the branch fracture, when the concentration of the anti-swelling agent is 0 wt%, the content of expandable shale particles is higher. The shedding and discharge of expanded shale particles can increase the fracture conductivity from 0.09 D·cm to 0.11 D·cm, and the cumulative oil can increase from 400 m^3 to 837 m^3. When the concentration of the anti-swelling agent is 2 wt%, the content of expandable shale particles is lower. The shedding and discharge of expanded shale particles can increase the fracture conductivity from 0.46 D·cm to 0.55 D·cm, and the cumulative oil can increase from 994 m^3 to 2116 m^3. For the major fracture, a similar law exists. When the concentration of the anti-swelling agent is 2 wt%, the shedding and discharge of expanded shale particles increases the conductivity of the fracture from 2.80 D·cm to 4.96 D·cm, and the cumulative oil increases from 6073 m^3 to 6898 m^3. However, when the concentration of the anti-swelling agent is 0 wt%, the cumulative oil with the shedding of hydrated and expanded shale particles is larger than that without shale shedding in the early stage of production. For the former case, with the increase of the production time, most of the hydrated and expanded shale particles in the fracture are produced first, and the conductivity of the fracture increases dramatically from 1.36 D·cm to 9.38 D·cm. However, the final cumulative oil decreases from 4640 m^3 to 4311 m^3. This is because of the large pressure drop formed in the shale matrix near the fracture, which can significantly reduce the shale porosity and permeability. At the same

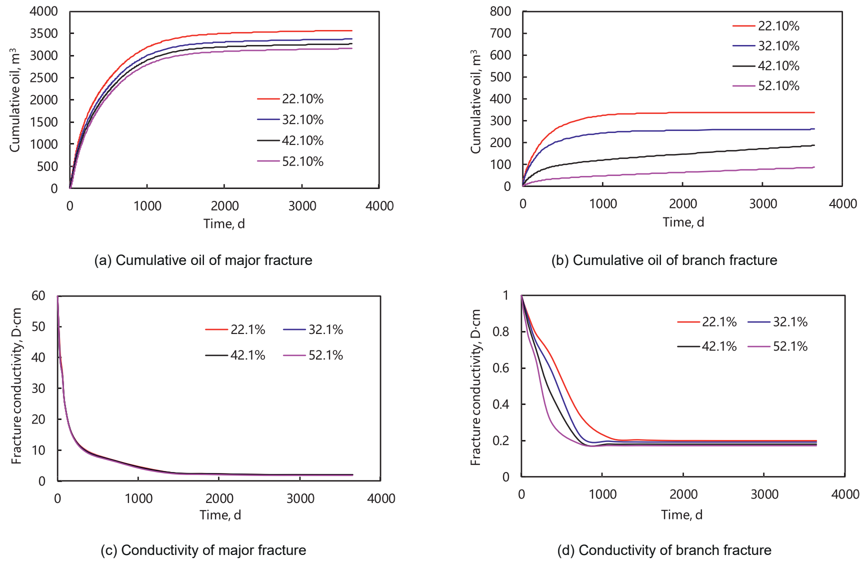

Fig. 8. Comparison of cumulative oils and fracture conductivities at different water saturations.

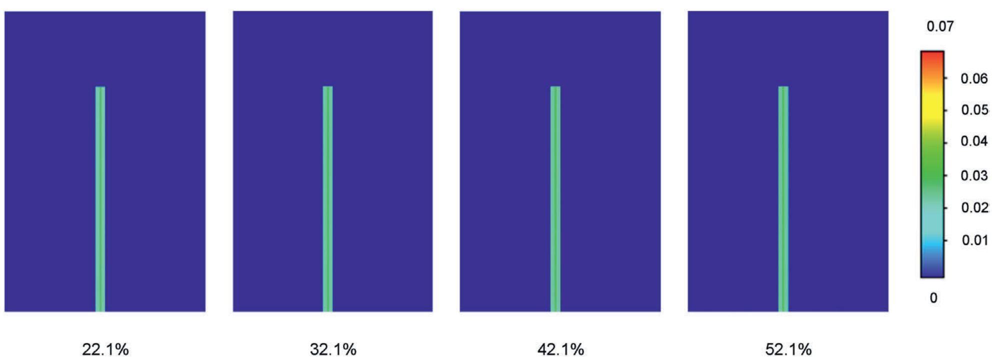

Fig. 9. Comparison of contents of deposited gel-breaking residue at different water saturations (unit: mol/m^3; taking major fracture as an example).

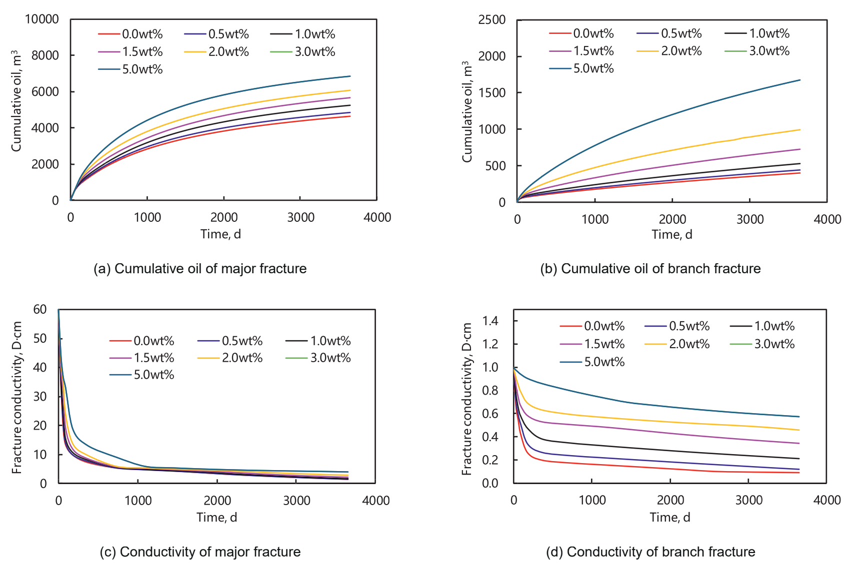

Fig. 10. Comparison of cumulative oils and fracture conductivities at different concentrations of anti-swelling agent in water.

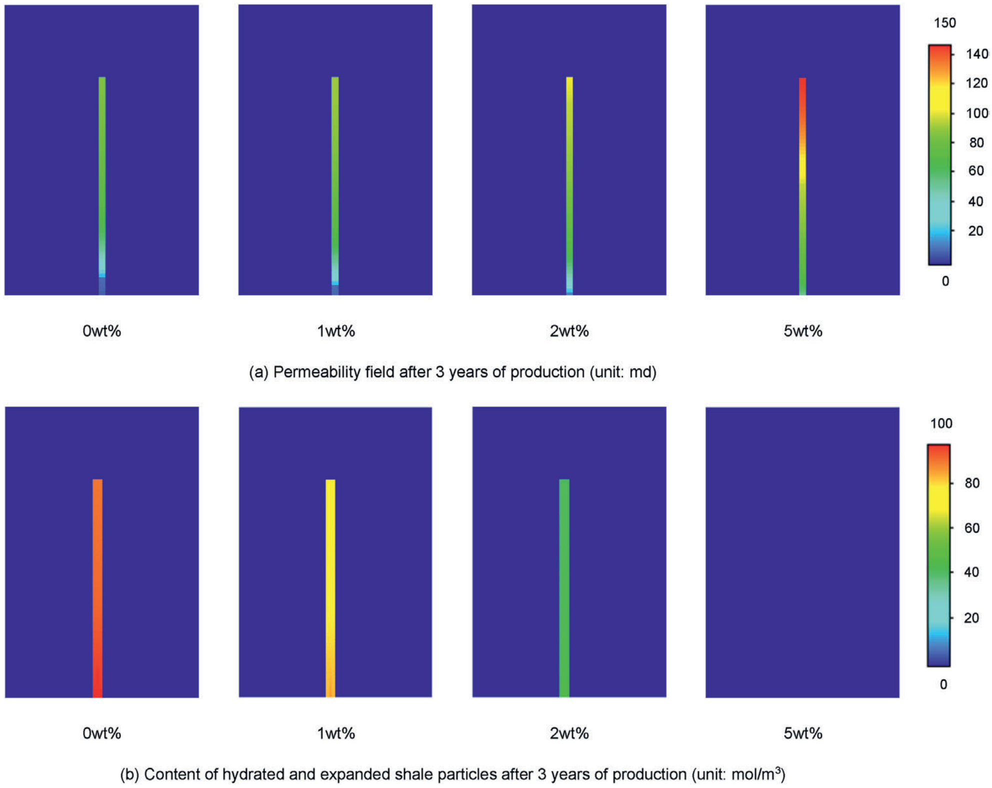

Fig. 11. Comparison of reservoir permeabilities and contents of hydrated and expanded shale particles in fractures at different concentrations of anti-swelling agents in water (taking major fracture as an example).

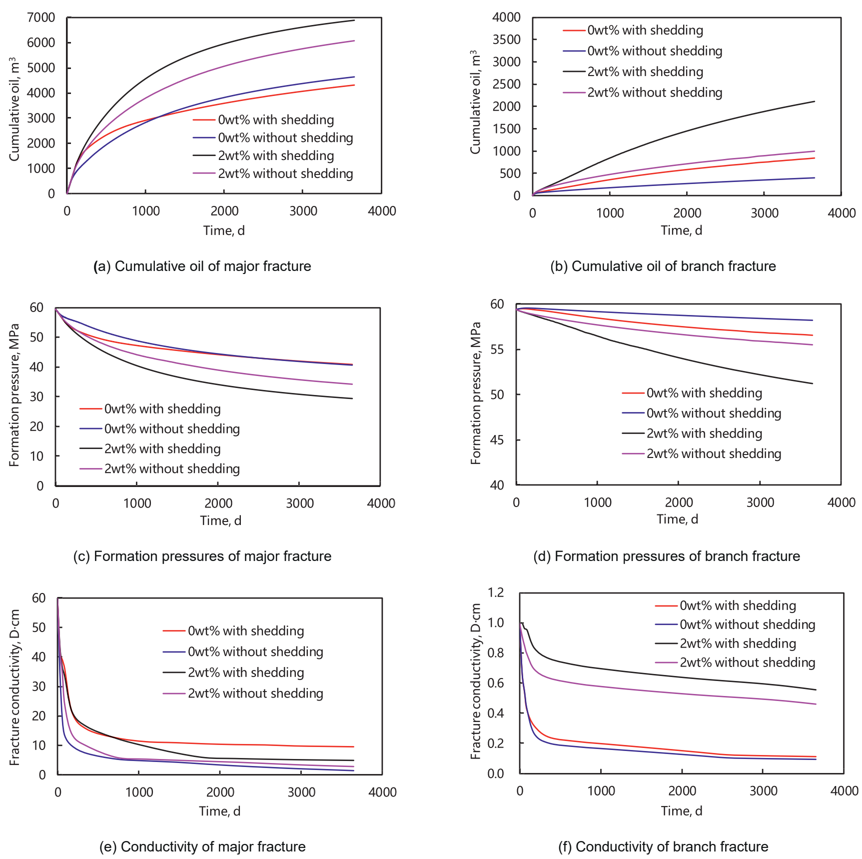

Fig. 12. Comparison of cumulative oils, formation pressures, and fracture conductivities with and without shale particle shedding at different anti-swelling agent concentrations.

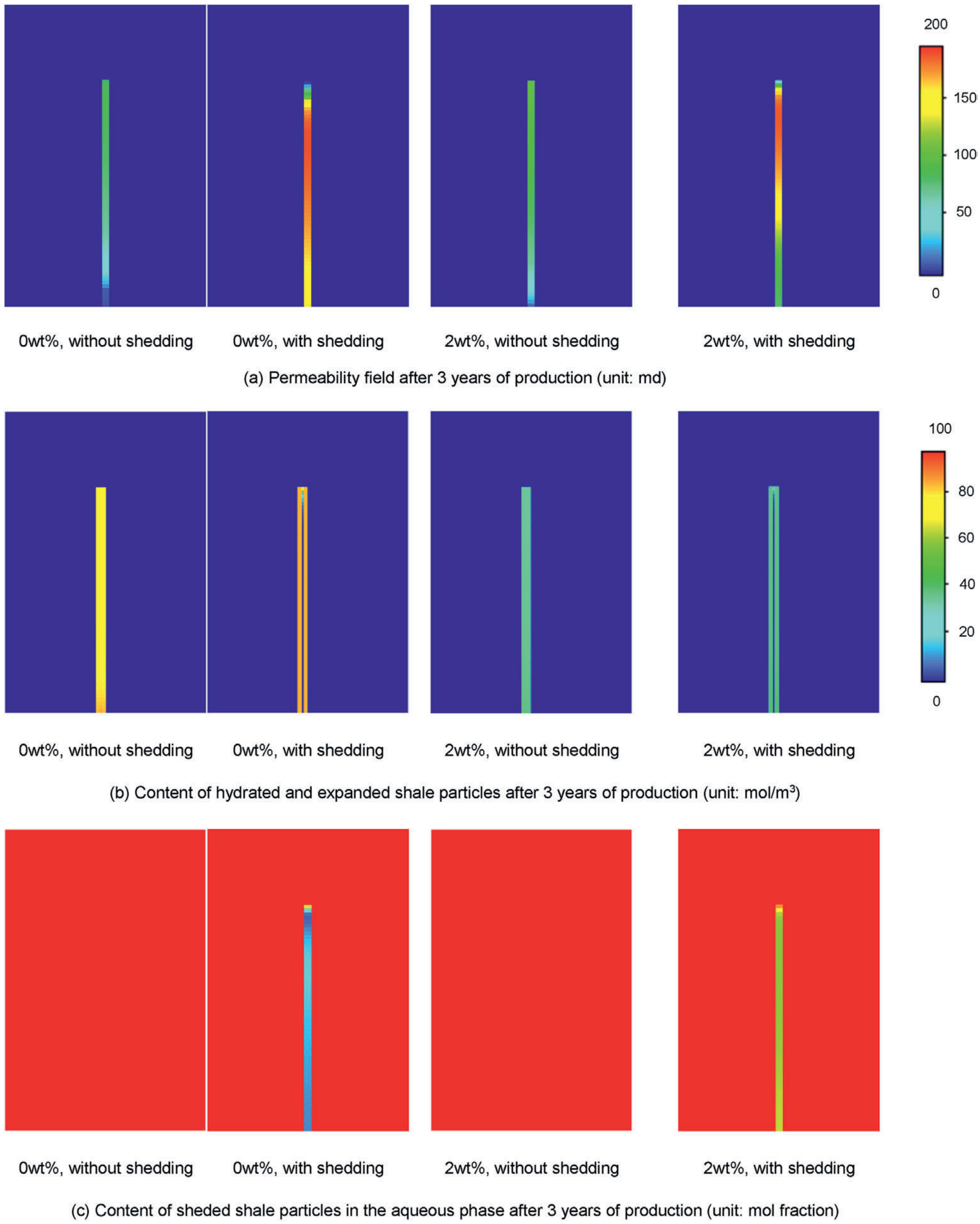

Fig. 13. Comparison of reservoir permeabilities and contents of different shale particles with and without shale particle shedding at different anti-swelling agent concentrations (taking major fracture as an example).

time, an increase in the water saturation and the content of the expanded shale particles can also be observed. This phenomenon can significantly restrict the flow of crude oil from the nearby matrix to the fracture. Therefore, in general, when the expanded shale particles are shed and discharged, the fracture conductivity will be restored to some extent, and the cumulative oil will also increase. However, it should be noted that the cumulative oil is also affected by the degree of damage to the porosity and permeability of the shale matrix near the fracture.

4.3.3. Influence of deposition and blockage of shedding shale particles

4.3.3.1. Influence of reaction frequency factor of shale particle deposition. Based on the shedding of shale particles, the damage mechanism of the shale particle deposition and blockage was further simulated and analyzed. Under the basic condition with an anti-swelling agent concentration of 2 wt%, the cumulative oil and related fracture parameters were compared at different deposition reaction frequency factors of shale particles. The results are shown in Figs. 14 and 15.

Through analysis, it can be seen that when the expanded shale particles are shed and deposited inside the fracture, it will cause the blockage of fracture and decrease the cumulative oil. Specifically, as the deposition reaction frequency factor of shale particles increases from 0 to 0.1 m^3/s/mol, the amount of shale particles deposited inside the fracture gradually increases. For the major fracture, the conductivity decreases from 4.96 D·cm to 2.72 D·cm, and the cumulative oil decreases from 6898 m^3 to 6038 m^3. For the branch fracture, the conductivity decreases from 0.55 D cm to 0.46 D cm, and the cumulative oil will decrease from 2116 m^3 to 994 m^3. The damage to fracture conductivity by shale particle deposition tends to stabilize when the deposition reaction frequency factor of

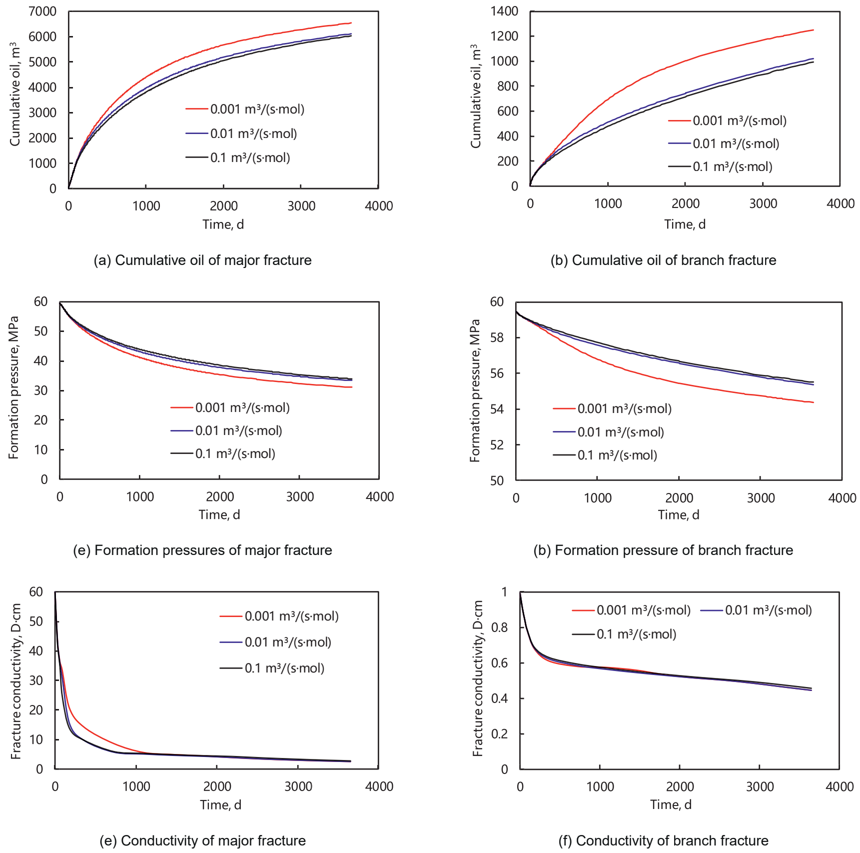

Fig. 14. Comparison of cumulative oils, formation pressures and fracture conductivities at different deposition fraction frequency factors of shale particle.

shale particles exceeds 0.01 m^3/s/mol. By comparison, it is found that the deposition and blockage process of shed shale particles is the opposite process of shedding and discharging of expanded shale particles. The former decreases the fracture conductivity and cumulative oil, while the latter increases the fracture conductivity and cumulative oil. If the reaction frequency factors of these two processes are the same, the overall performance is an increase in fracture conductivity and cumulative oil. If the effects of these two processes on fracture conductivity and cumulative oil cancel each other out, the deposition reaction frequency factor of shale particles should be larger than that of the shedding process (e.g., 0.1 m^3/s/mol for the former and 0.001 m^3/s/mol for the latter).

4.3.3.2. Influence of critical water velocity for shale particle shedding. The critical water flow velocity significantly affects the amount of shed shale particles and can further affect the deposition and blockage risk of shale particles in the fracture. Hence, under the basic condition with an anti-swelling agent concentration of 2 wt%, the cumulative oil and related fracture parameters were compared at different critical water flow velocities for shale particle shedding. The results are shown in Figs. 16 and 17.

The analysis shows that as the critical water flow velocity of shale particles increases from 0.001 m/d to 1 m/d, the conductivity of major fracture increases from 2.14 D·cm to 2.78 D·cm, and the cumulative oil increases from 6030 m^3 to 6557 m^3; the conductivity of branch fracture increases from 0.44 D·cm to 0.51 D·cm, and the cumulative oil increases from 992 m^3 to 1375 m^3. The smaller the critical flow velocity is, the easier it is for the hydrated and expanded shale particles on the fracture wall to shed and flow back with the fracturing fluid to deposit in the fracture. When the critical flow velocity is greater than 0.1 m/d, it will exceed the actual water flow velocity within the fracture, and no shedding of shale particles from the fracture walls will occur. In this case, the concentration of shale particles deposited in the fracture is close to zero.

4.4. Influence of coupling mode of damage mechanisms on fracture conductivity and oil production

Based on the case without fracture conductivity damage, the fracture damage mechanisms, including stress sensitivity, deposition of gel breaking residue, shale particle hydration and expansion, shedding, and deposition, were sequentially activated in the simulation model, and the main simulation results are shown in Figs. 18 and 19.

It can be seen that with the sequential superposition of various fracture damage mechanisms, the change process of the major fracture conductivity is 60 D·cm → 3.57 D·cm → 2.1 D·cm → 1 D·cm → 2.15 D·cm → 2 D·cm with a final decrease of 96.67%, and the change process of cumulative oil is 7432 m^3 → 6654 m^3 → 3570 m^3 → 2564 m^3 → 4084 m^3 → 3257 m^3 with a final drop of 56.18%; the change process of the branch fracture conductivity is 1 D·cm → 0.57 D·cm → 0.2 D·cm → 0.19 D·cm → 0.21 D·cm → 0.1 D·cm with a final decrease of 90%, and the change process of cumulative oil is 4917 m^3 → 1560 m^3 → 339 m^3 → 271 m^3 → 349 m^3 → 243 m^3 with a final drop of 95.06%. The overall trend of the fracture conductivity and cumulative oil is decreasing with the sequential superposition of various fracture damage mechanisms. When the damage mechanisms are superposed to the hydrated and expanded shale particles to be shed and discharged, it plays a

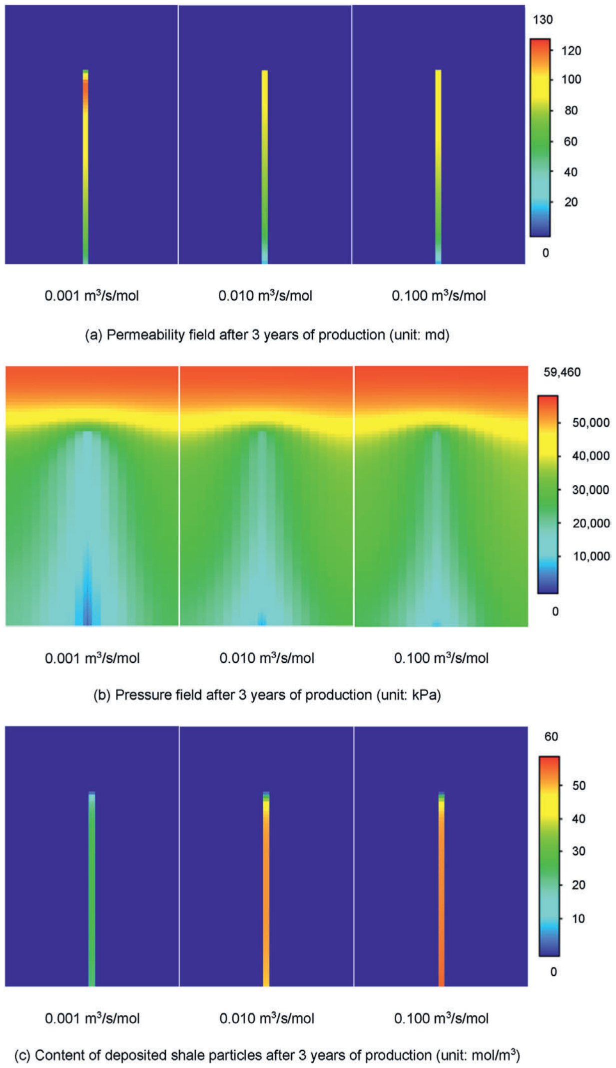

Fig. 15. Comparison of reservoir permeabilities, formation pressures, and contents of deposited shale particles at different deposition reaction frequency factors of shale particles (taking major fracture as an example).

blockage removal effect. Especially for the major fracture, the fracture conductivity and cumulative oil recover remarkably. Overall, because the initial permeabilities and stress sensitivities of major and branch fractures are different, the decrease in conductivity of major fracture is relatively large, but the decrease in cumulative oil is relatively small, whereas the opposite is true for branch fracture, and the damage of branch fracture has a more significant effect on cumulative oil.

5. Discussion

In this study, the understanding of the damage mechanism of fracture conductivity in shale oil reservoirs is deepened. The decline in fracture conductivity is the result of a combination of different damage mechanisms. In the actual field, the damage mechanisms of fracture conductivity may be more complex than the conditions involved in this study. It should be analyzed according to the specific conditions. The results of this study show that the decrease in oil production is mainly affected by fracture stress sensitivity and is also related to the degree of contamination of the fracture wall. The deposition of the gel-breaking residue and the hydration expansion of the clay minerals in the pores of the fracture wall affect the flow of crude oil from the shale matrix to the fracture. However, these two damages can be minimized by reducing the content of the gel-breaking residue and improving the inhibitory effect of the anti-swelling agent in the fracturing fluid. The shedding of the hydrated and expanded shale particles from the fracture walls can help to remove the blockage on the fracture walls. However, it is not sure whether the shed shale particles can flow out of the fracture efficiently with the oil and water. Especially in the complex fracture network system, the shale particles are easily retained in the intersections and transitions of the fracture and thus form a blockage.

The understanding gained from this study can bring some inspiration to the design of the fracture conductivity, the selection of the fracturing fluid, and the optimization of the production parameters. In the simulation, the conductivity along the whole fracture was set to be the same at the beginning, which is equal to the assumption that the proppant is evenly distributed in the fracture. In this case, under the large pressure drop near the well, the conductivity of the fracture near the well will decline much more greatly than that in the fracture far away from the well. Especially for the branch fracture with a low sanding concentration, it is easier to cause the fracture near the well to be closed, which is not conducive to pressure propagation and oil production. Therefore, when designing fracture conductivity, the change of effective closing pressure along the fracture and the decline of the fracture conductivity under the closing pressure should be taken into account. A reasonable non-uniform sanding concentration can maintain a high fracture conductivity during the whole process of oil production (Zhou et al., 2023). For the formulation of fracturing fluids, in addition to meeting the basic requirements for sand carrying, its reservoir protection effect should also be improved, such as reducing the content of the gel-breaking residue and selecting high-performance anti-swelling agents to avoid shale hydration and expansion. In recent years, the function of enhanced oil recovery (EOR) of fracturing fluid in the shale oil reservoir has gradually attracted more and more attention. It considers adding some surface-active substances to the fracturing fluid to reduce the interfacial tension between oil and water and to enhance the imbibition effect of fracturing fluid to replace oil. This has been widely applied during the process of hydraulic fracturing in low-permeability and tight sandstone reservoirs. However, whether it can be effective in the nano-scale pores of shale with complex wettability needs further in-depth research (Palla et al., 2014). In addition, based on the reasonable characterization of the damage mechanism of the fracture conductivity, the performance of depressurization for production and gas injection for EOR in a real fracture system should be further investigated. The measures to reduce the influence of various damage mechanisms on fracture conductivity and oil production will be also explored in the future (Xu et al., 2021).

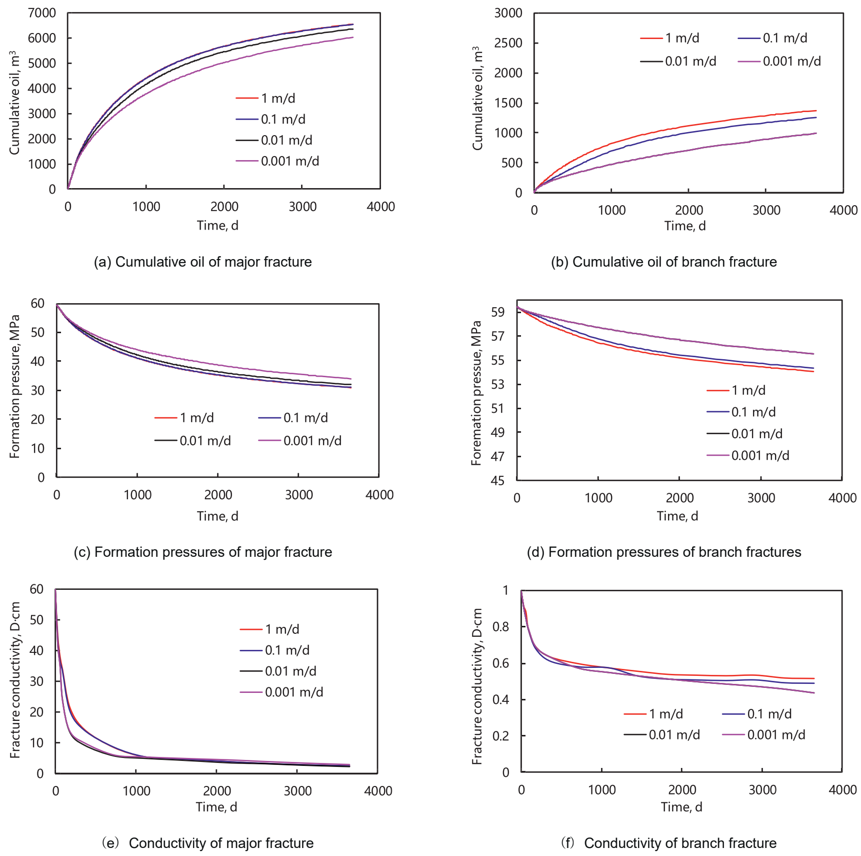

Fig. 16. Comparison of cumulative oils, formation pressures, and fracture conductivities at different critical water flow rates for shale particle deposition.

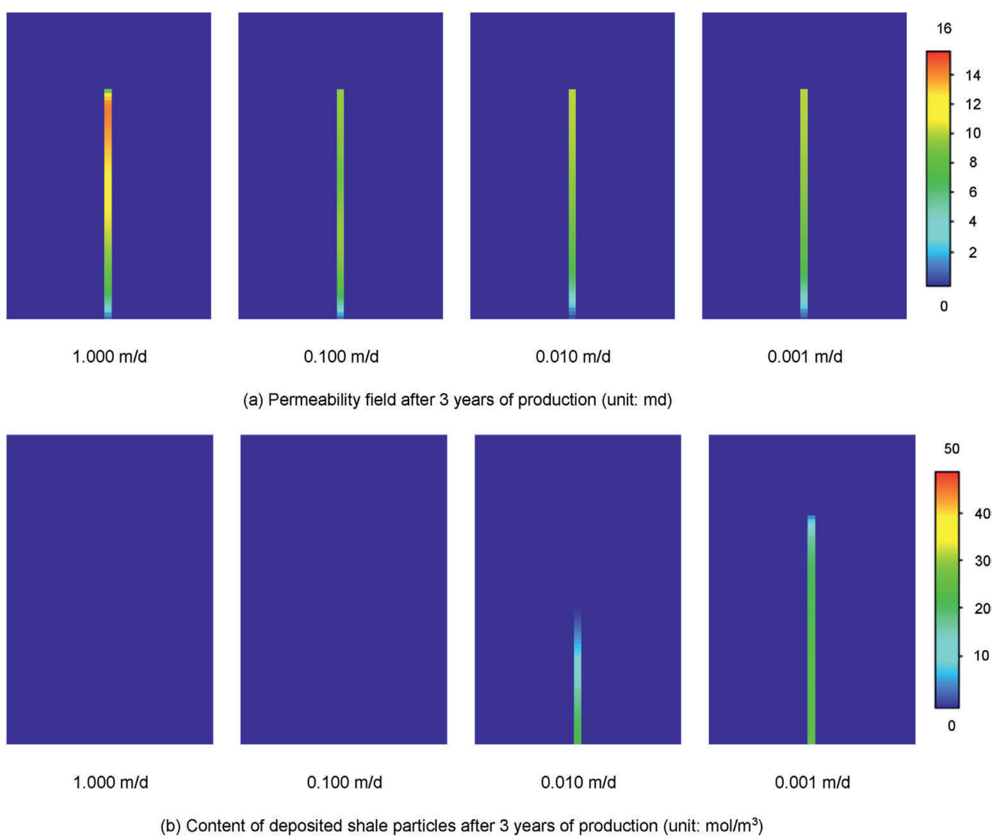

Fig. 17. Comparison of reservoir permeabilities, and contents of deposited shale particles at different critical water flow rates for shale particle deposition (taking major fracture as an example).

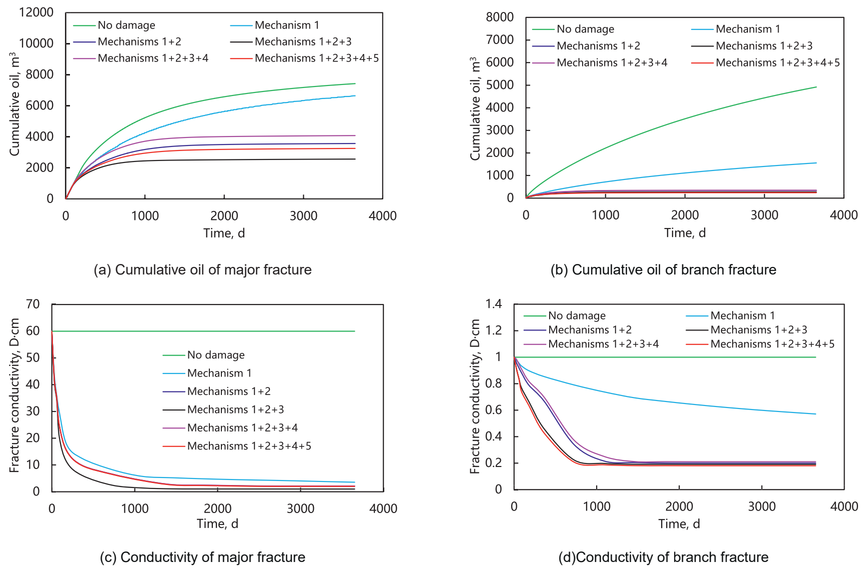

Fig. 18. Comparison of cumulative oils and fracture conductivities under different coupling modes of damage mechanisms.

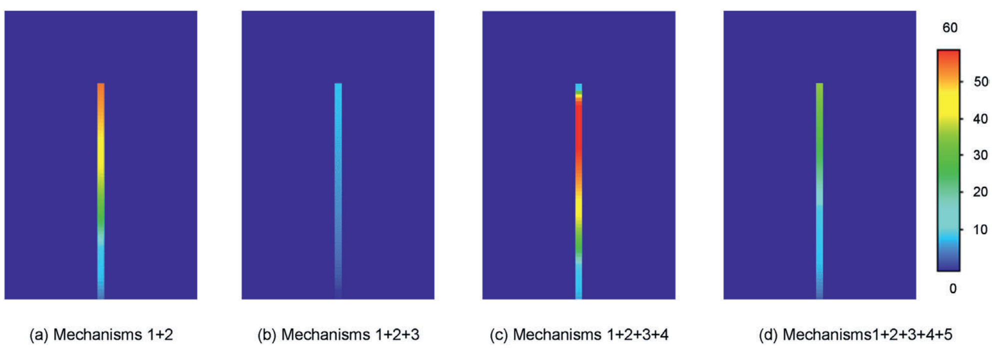

Fig. 19. Comparision of permeability fields after 3 years of production under different coupling modes of damage mechanisms (unit: md; taking major fracture as an example).

6. Conclusion

(1) The damage mechanism model of fracture conductivity in shale oil reservoirs proposed in this study considers most of the important damage mechanisms in fracture, and a corresponding numerical simulation model was established to conduct the sensitivity analysis of influencing factors. The fracture stress sensitivity can be characterized by a porosity-permeability relationship table, and the deposition of gel-breaking residue and the hydration-expansion-shedding-deposition process of shale particles can be described using the reaction kinetic equations.

(2) The sensitivity analysis shows that the fracture conductivity and oil production will decrease gradually when different fracture damage mechanisms are sequentially superimposed. For the major fracture, the conductivity and oil production can decrease by 96.67% and 56.18%, respectively, while for the branch fracture, they can decrease by 90% and 95.06%, respectively. Stress sensitivity is the primary fracture damage mechanism. The damage of stress sensitivity of branch fracture is much stronger than that of primary fracture. The decline of oil production is also affected by the contamination of the fracture wall caused by the deposition of gel-breaking residue and the hydration and expansion of shale particles. The shedding and discharging of these shale particles can facilitate the restoration of fracture conductivity, but if these shale particles deposit in the fracture, it will cause secondary damage again.

(3) In the field, the actual fracture system of shale oil reservoirs is more complex. The decrease of conductivity and oil production is usually the result of the combined action of various damage mechanisms, which should be analyzed according to the specific situation. The understanding in a single fracture gained from this study can bring some inspiration to the design of fracture conductivity, the preference of fracturing fluid, and the optimization of production parameters. The research based on the real fracture morphology should be carried out in the future.

CRediT authorship contribution statement

Liang Zhang: Writing – review & editing, Validation, Methodology, Conceptualization. **Runzhen Wu:** Writing – review & editing, Writing – original draft, Validation. **Chuan He:** Writing – review & editing, Validation, Methodology, Investigation, Conceptualization. **Xiang Li:** Investigation, Conceptualization. **Yige Qi:** Investigation, Conceptualization. **Linchao Yang:** Investigation. **Zilin Zhang:** Validation, Investigation.

Declaration of competing interest

The authors declare that there is no conflict of interest.

Acknowledgments

This work is supported by the Shengli Oilfield Branch, Sinopec (project no. 30200002-21-FW2099 -0088). It is also financed by the National Major Science and Technology Project for New Exploration and Development of Oil and Gas (2025ZD1404404-04). We also appreciate the reviewers and editors for their constructive comments to make the paper high-quality.

References

Ahamed, M.A.A., Perera, M.S.A., Black, J.R., Matthai, S.K., Ranjith, P.G., Li, D.Y., Sampath, K.H.S.M., 2021. Investigating the proppant damage mechanisms expected in a propped coal fracture and its effect on fracture flow. J. Petrol. Sci. Eng. 198, 108170.

Chalmers, G., Ross, D., Bustin, R., 2012. Geological controls on matrix permeability of Devonian gas shales in The Horn river and Liard basins, northeastern British Columbia, Canada. Int. J. Coal Geol. 103, 120–131.

Chen, Z., Liu, H.L., Li, Y.J., Shen, Z.Q., Xu, G.Q., 2021. The current status and development suggestions for shale oil reservoir stimulation at home and abroad. Petrol. Drill. Techn. 49 (4), 1–7.

Cho, Y., Apaydin, O.G., Ozkan, E., 2013. Pressure-dependent natural-fracture permeability in shale and its effect on shale-gas well production. SPE Reservoir Eval. Eng. 16 (2), 216–228.

Ci, X.H., Lv, M.M., Ma, G.Q., Niu, Q., 2020. Research on shale oil logging evaluation method and its application in Shengli oil zone. In: International Conference on Oil and Gas Field Exploration and Development. Chengdu.

Cui, Y.Z., Zhang, F.B., Jiang, R.Z., Lin, J.Q., 2022. Pressure transient behavior modeling of a multi-horizontal well pad with damaged fracture in shale gas. J. Petrol. Sci. Eng. 216, 110755.

Ding, X.M., 2013. The Effect of Stress-dependent Permeablity on Sandstone Gas Well Testing and Production Decline. China University of Geosciences, Beijing.

He, C., Wen, R.H., Liang, Y.Z., Zhang, D., Zhang, L., 2022. Prediction model of fracture conductivity and analysis of influencing factors in shale oil reservoirs. In: International Conference on Exploration and Development of Oil and Gas Fields. Urumqi.

Jia, C.G., 2014. Evaluation on conductivity performance of proppant in shale gas network fracturing. Petrol. Drill. Techn. 42 (5), 42–46.

Jiao, K.T., Han, D.X., Wang, D.B., Chen, Y.J., Li, J.F., Gong, L., Bai, B.F., Yu, B., 2022. Investigation of thermal-hydro-mechanical coupled fracture propagation considering rock damage. Comput. Geosci. 26, 1167–1187.

Katende, A., Allen, C., Rutqvist, J., Nakagawa, S., Radonjic, M., 2023. Experimental and numerical investigation of proppant embedment and conductivity reduction within a fracture in the Caney Shale, Southern Oklahoma, USA. Fuel 341, 127571.

Kong, D.B., Gao, J.D., Zhu, W.Y., Yue, M., Li, H.S., 2022. Experimental study on conductivity and stress sensitivity of fully supported fractured shale cores. J. Petrol. Sci. Eng. 218, 110971.

Li, R.S., Li, H.B., Yang, Z.M., Guo, H.K., Gao, T.N., Dai, X.Y., Meng, H., 2019. Experimental study on stress sensitivity of shale oil reservoir. Chin. Sci. Paper 14 (9), 969–974.

Li, H.L., Lu, Y.Y., Zhou, L., Han, S.B., Gou, Y., 2017. A new constitutive model for calculating the loading-path dependent proppant deformation and damage analysis of fracture conductivity. J. Nat. Gas Sci. Eng. 46, 365–374.

Li, W.G., Zhong, B., Zhang, X.T., Hu, Z.M., Xie, L.L., 2016. Evaluating method of the stress sensitivity for the artificial fractures in the shale. Daqing Petrol. Geol. Dev. 35 (3), 159–164.

Liu, W., Chen, Y.F., Hu, R., Zhou, W., Zhou, C.B., 2016. A two-step homogenization-based permeability model for deformable fractured rocks with consideration of coupled damage and friction effects. Int. J. Rock Mech. Min. Sci. 89, 212–226.

Liu, Y.K., Wang, F.J., Wang, Y.M., Li, B.H., Zhang, D., Yang, G., Zhi, J.Q., Sun, S., Wang, X., Deng, Q.J., Xu, H., 2022. The mechanism of hydraulic fracturing assisted oil displacement to enhance oil recovery in low and medium permeability reservoirs. Petrol. Explor. Dev. 49 (4), 752–759.

Liu, K., Zhang, S.Q., 2015. Developmental justice critique of contemporary shale gas revolution. J. Nanjing Univ. Technol. (Nat. Sci. Ed.) 14 (1), 15–21.

Meng, Y., Wang, Z.L., Zhang, L.Y., He, C., Wen, R.H., Zhang, L., 2021. Experimental evaluation on the conductivity of branch fracture with low sand laying concentration and its influencing factors in shale oil reservoirs. Lithosphere S1, 4500227.

Ni, X.M., Yu, Y.Y., Cao, Y.X., 2016. Study on changing characteristics about proppant flow conductivity under the influence of HPG fracturing fluid. Coal Sci. Technol. 44 (3), 86–90.

Palla, C., Weaver, J.D., Benoit, D., Lu, Z., Vera, N., 2014. Impact of surfactants on fracture fluid recovery. In: The Abu Dhabi International Petroleum Exhibition and Conference. Abu Dhabi, UAE.

Peng, Y., Luo, A., Li, Y.M., Wu, Y.J., Xu, W.J., Sepehrnoori, K., 2023. Fractional model for simulating long-term fracture conductivity decay of shale gas and its influences on the well production. Fuel 351, 129052.

Reyes, L., Osisanya, S.O., 2002. Empirical correlation of effective stress dependent shale rock properties. J. Can. Petrol. Technol. 41 (12). PETSOC-02-12-02.

Shi, Y.J., Sun, X.P., 2001. Stress sensitivity analysis of changqing dense clastic reservoir. Petrol. Explor. Dev. (5), 85–87.

Sun, S.D., 2013. Experimental study on the effect of reservoir physical properties on pressure sensitivity of low-permeability reservoirs. J. Oil Gas Technol. (J. Jianghan Petroleum Inst.) 35 (3), 118–121+167.

Wang, J., Huang, Y.X., Zhang, Y., Zhou, F.J., Yao, E.D., Wang, R., 2020a. Study of fracturing fluid on gel breaking performance and damage to fracture conductivity. J. Petrol. Sci. Eng. 193, 107443.

Wang, J., Huang, Y.X., Zhou, F.J., Liang, X.Y., 2020b. The influence of proppant breakage, embedding, and particle migration on fracture conductivity. J. Petrol. Sci. Eng. 193, 107385.

Xu, Z., Peng, N.J., Shi, W.Z., Su, Z.G., 2021. Characteristics of fracture and its controlling factors in shale gas reservoirs of Wufeng-Longmaxi Formation in Fuling area. J. Donghua Univ. Sci. Technol. (Nat. Sci. Edit.) 44 (3), 267–279.

Xue, D., Zhang, S.A., Wu, X.M., Li, X.H., Du, J.J., Lu, C.G., 2019. Sensitivity experiment of shale gas reservoir of Chang 7 reservoir in Xiasiwan oilfield. Litholog. Reserv. 31 (3), 135–144.

Yin, B., Zhang, Y., Lou, Y.S., Liu, S.Y., 2025. Damage mechanism of proppant and conductivity reduction post fracturing in unconventional reservoirs. Fuel 380, 133086.

Zhang, J.J., Zhu, D., Hill, A.D., 2015. A new theoretical method to calculate shale fracture conductivity based on the population balance equation. J. Petrol. Sci. Eng. 134, 40–48.

Zhou, J., Zhang, X.D., Zhou, L.B., 2023. Experimental study on improving the fracture conductivity of acid etched fracture for ultra-deep and high stress carbonate reservoirs. In: The 57th U.S. Rock Mechanics/Geomechanics Symposium, Atlanta, Georgia, USA.